Groundwater for Sustainable Development 27 (2024) 101318

Contents lists available at ScienceDirect

Groundwater for Sustainable Development

journal homepage: www.elsevier.com/locate/gsd

Research paper

Effectiveness of different mixed physical barriers in controlling seawater intrusion in homogeneous and layered coastal aquifers

Ismail Abd-Elaty [a,**], Alban Kuriqi [b], Ashraf Ahmed [c,*]

[a] Department of Water and Water Structures Engineering, Faculty of Engineering, Zagazig University, Zagazig, 44519, Egypt
[b] CERIS, Instituto Superior Técnico, Universidade de Lisboa, Av. RoviscoPais 1, 1049-001, Lisbon, Portugal
[c] Department of Civil and Environmental Engineering, Brunel University London, Kingston Lane, Uxbridge, UB83PH, United Kingdom

HIGHLIGHTS

- Salt repulsion is mitigated by installing permeable walls and impermeable dams.
- Up to 92% SWI removal for layered aquifers using a mixed physical barrier.
- Salt removal in the homogenous Biscayne aquifer was consistent with the lab-scale results.

GRAPHICAL ABSTRACT

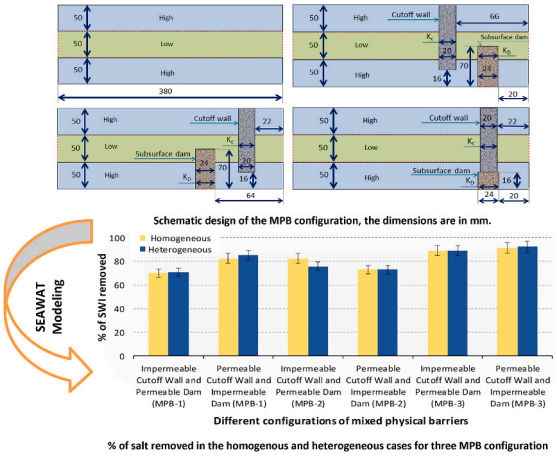

% of salt removed in the homogenous and heterogeneous cases for three MPB configuration

ARTICLE INFO

Keywords:
Aquifer desalinization
Climate change
Coastal aquifer management
Cut-off wall
Freshwater decontamination

ABSTRACT

The intrusion of salt water into coastal regions threatens water resources, especially in arid and semi-arid regions. It damages large quantities of fresh water in these regions, and the productivity of the freshwater abstraction wells declines. Management of seawater intrusion (SWI) is therefore needed to improve fresh groundwater in these regions. This study investigated 12 different configurations of mixed physical subsurface barriers (MPBs) to control SWI in homogeneous and heterogeneous layered aquifers. The effectiveness of different MPB locations and configurations was tested, including (i) a barrier wall on the landward side and the subsurface dams on the seaward side, (ii) a barrier wall on the seaward side and a subsurface dam on the landward side, and (iii) the barrier wall was placed above the subsurface dam, both with different permeabilities. All simulations were based on the SEAWAT code. The numerical model was validated against experimental data. The results showed that a permeable cut-off wall above an impermeable subterranean dam (case MPB-3) with

* Corresponding author.
** Corresponding author.
E-mail addresses: Eng_abdelaty2006@yahoo.com, Eng_abdelaty@zu.edu.eg (I. Abd-Elaty), alban.kuriqi@tecnico.ulisboa.pt (A. Kuriqi), ashraf.ahmed@brunel.ac.uk (A. Ahmed).

https://doi.org/10.1016/j.gsd.2024.101318
Received 8 March 2024; Received in revised form 9 August 2024; Accepted 17 August 2024
Available online 20 August 2024

different permeabilities resulted in a reduction of the seawater wedge of 91% and 92% for homogeneous and heterogeneous layered aquifers, respectively. When the barrier wall was placed on the land side and the dam on the seaside (case MPB-1), the reduction of the seawater wedge reached 83% and 85% for homogeneous and heterogeneous layered aquifers, respectively. In contrast, when the dam was placed on the land side and the wall on the seaside (case MPB-2), the saltwater wedge was reduced by 73% for both homogeneous and heterogeneous layered aquifers. In addition, a case study was conducted on the Biscayne aquifer, southeast Florida, USA, with homogeneous conditions. Seawater intrusion was reduced by 36% and 44% in case MPB-1, 41% and 38% in case MPB-2, and 43% and 46% in case MPB-3. These seawater intrusion control methods offer numerous benefits, including improving freshwater storage, effectively controlling salinity during droughts, and potentially improving contaminant management.

Acronyms

IMT	Integrated MT3DMS Transport process
MODFLOW	United States Geological Survey modular finite-difference groundwater flow
MPB	mixed physical subsurface barriers
MT3DMS	A modular three-dimensional multispecies transport model
PSBs	Physical subsurface barriers
SWI	Saltwater intrusion
SEAWAT	Three-dimensional variable-density groundwater flow and transport model
VDF	variable density flow process

1. Introduction

Freshwater scarcity is the major challenge that many countries around the world are facing (Cooley et al., 2014; Abd-Elaty and Zelenakova, 2022). Freshwater resources in hyper-arid and arid areas are in shortage compared to humid and wet regions. The movement of saline water can cause freshwater contamination in coastal aquifers. The landside fresh groundwater boundaries accelerate groundwater salinity in coastal areas due to increased abstraction, decreased recharge, and increased saline water heads (Abd-Elaty and Zelenakova, 2022). Seawater intrusion into coastal aquifers can increase groundwater salinity beyond potable levels, endangering access to freshwater for millions of people level (Jasechko et al., 2020). The availability of clean groundwater in the coastal aquifer is critical for future development. However, policymakers face significant difficulties in addressing this issue. Groundwater in coastal arid regions is under increasing pressure due to rapid population growth, intensive agriculture, and climate change (Ranjan et al., 2006). Saltwater intrusion is a phenomenon due to the high density of saline water and the low density of fresh groundwater, which increases aquifers' salinity and includes groundwater resource depletion (Abd-Elaty et al., 2023a). The coastal areas worldwide are at high risk of SWI (Ashrafuzzaman et al., 2022; Rizzo et al., 2022).

Currently, the most common mitigation measures for SWI are (i) optimization of well locations, (ii) natural and artificial recharge, (iii) saline water abstraction, (iv) land reclamation, and (v) physical subsurface barriers (Tansel and Zhang, 2022; Elaty and Polemio, 2023). Despite their high construction cost, the physical subsurface barriers (PSBs) are an effective method and practical solution to tackle SWI in coastal aquifers (Allow, 2011). PSBs are constructed parallel to the coast and are either permeable or semi-permeable structures (Abdoulhalik et al., 2017). PSBs are impermeable or semi-permeable structures placed along the coastal aquifer to increase the fresh groundwater storage capacity (Abd-Elaty et al., 2019). Based on the design specifications, PSBs are generally classified as either cut-off walls or subsurface dams. Each of these serves a distinct purpose.

Cut-off walls are installed perpendicular to the aquifer flow direction; the dam is embedded in the aquifer bedrock, as are storage dams (Roger et al., 2010). Cutoff walls are designed to extend from the top of the aquifer to a predefined depth, acting as barriers to the lateral flow of groundwater. Dams act as subsurface storage dams, with a base embedded in the aquifer bedrock and an open crest at the upper part of the aquifer, allowing groundwater to percolate through the dam (Luyun Jr, K. Momii., 2011). Barsi (2001) optimized the construction cost of the subsurface barrier through the width and location and showed that the subsurface dam function is increased by the groundwater storage and retard SWI by rainfall harvesting and recharge into the coastal aquifers.

The subsurface dam's advantages include less reduction of storage capacity due to silting, low evaporation losses, maintaining water quality, less susceptibility to pollution and health hazards, minimal risk of the dam collapse, low construction cost, and capability to adjust the dam's hydraulic conductivity due to requirements. The disadvantages include low downstream flow, which may lead to land subsidence and/or seawater intrusion, increasing soil pore pressure, and uplift pressure on the infrastructures (Elaty and Polemio, 2023; Abdoulhalik and Ahmed 2017a) also studied the effectiveness of cutoff walls in layered heterogeneity using numerical and experimental procedures. A low permeability layer at the middle or bottom of the aquifer inhabited the wall's ability to effectively control SWI. On the other hand, when the low permeability existed at the top of the aquifer, it enhanced the effectiveness of the cutoff wall as a SWI control method. Abdoulhalik et al. (2017b) investigated the effectiveness of subsurface dams in layered heterogeneous soil. The aquifer stratification extended the cleanup time from SWI contamination, particularly when a low hydraulic conductivity layer existed at the bottom of the aquifer. Among these methods, PSBs offer several advantages compared to other solutions, such as better control of groundwater levels and aquifer management, relatively low environmental impact, long-term effectiveness, and flexibility to various geological and hydrological conditions (Allow, 2011; Chang et al., 2019).

Many studies have reported the abilities of the PSBs to control SWI by using groundwater models under different climate changes in humid and hyper-arid regions (Harne et al. (2006); Abd-Elaty and Zelenakova (2022)). The results showed that the cut-off wall provided superior SWI mitigation compared to the dam. Researchers concluded that PSBs and hydraulic methods effectively reduced SWI in hyper-arid and arid regions. One of the few studies examined the effectiveness of physical barriers in layered heterogeneous aquifers (Abdoulhalik and Ahmed, 2017). A low hydraulic conductivity interlayer showed the capability of cut-off walls to block and repel saltwater intrusion (SWI) back effectively.

Moreover, a low hydraulic conductivity layer at the bottom of the aquifer could restrict the wall's ability to repel SWI. Abdoulhalik et al., (2017c) introduced an interesting idea of mixed physical barriers (MPB). The mixed physical barrier practices using an impermeable cut-off wall in conjunction with a semi-permeable subsurface dam as a new system to control seawater intrusion. In the past, cut-off walls and subsurface barriers have proven themselves as efficient solution in combating seawater intrusion; however, the results of using the two physical barriers in conjunction have not yet been explored. Abd-Elaty et al. (2024)

studied the impact of shoreline subsurface dams to protect from sea level rise and SWI. The study showed that this method is good for mitigating the coastal aquifers' salinity, increasing the freshwater storage at the coastal zones where the low salinity occurs, and reducing the freshwater supply cost. Yu et al. (2024) studied the impact of beach nourishment on SWI in layered heterogeneous aquifers. The study showed that beach nourishment of heterogeneous aquifers creates complex fresh-saline interface movement; also, it can merge layered heterogeneity and cause severe groundwater salinization.

Most of the previous studies have primarily investigated the SWI in coastal aquifers using physical subsurface barriers, such as cut-off walls, subsurface dams, or a mix of the two.

The combined use of impermeable walls and semi-permeable underground dams has only been researched to a limited extent to date. In particular, the interaction and combined effectiveness of these barriers in different aquifers have not been well-researched. The effects of mixed physical barriers in different configurations and their potential advantages over single barrier methods have not been sufficiently explored. The role of layered heterogeneity on the efficiency of subsurface dams and other physical barriers is not fully understood. Studies such as Abdoulhalik and Ahmed (2017b) have highlighted the variability in effectiveness, but comprehensive assessments across different geological settings are needed. More detailed studies are needed to understand how low hydraulic conductivity strata affect the performance of physical barriers in both homogeneous and layered heterogeneous aquifers. There is a need for comparative studies that evaluate the performance of different methods of SWI containment in different hydrogeologic settings. The development of best practice guidelines for the design, implementation, and management of physical barriers in coastal aquifers is needed to assist policymakers and engineers.

Thus, this study examined three different configurations of mixed physical barriers to find the optimal design and location of the barrier that best reduces the saline water wedge. Also, the current study investigated the efficiency of these mixed physical barriers in homogenous and layered heterogeneous aquifers. The physical barriers were also tested on the Biscayne aquifer, southeast Florida, USA, with homogeneous conditions.

2. Materials and method

2.1. Numerical analysis

The SEAWAT model was used in this study to simulate the spatial evolution of SWI. Specifically, a coupled version of the MODFLOW and MT3DMS (SEAWAT V4) was used to integrate the density-dependent flow and the solute transport equation (Langevin et al., 2020).

The variable density flow (VDF) process solves the variable density flow equation in terms of the freshwater head [Langevin, 2001] Eq. (1):

$$\nabla\left[\rho\frac{\mu_o}{\mu}K_o\left(\nabla h_0+\frac{\rho-\rho_o}{\rho_o}\nabla z\right)\right]=\rho S_{s,0}\left(\frac{\partial h_o}{\partial t}\right)+\theta\left(\frac{\partial \rho}{\partial C}\right)\left(\frac{\partial C}{\partial t}\right)-\rho_s q_s^{\backslash} \quad [1]$$

The Integrated MT3DMS Transport (IMT) process solves the solute transport equation (Zheng and Wang, 1999), Eq. (2):

$$\left(1+\frac{\rho_b K_d^k}{\theta}\right)\left(\frac{\partial(\theta C^k)}{\partial t}\right)=\nabla\left[\theta\left(D_m{}^k+\alpha\frac{q}{\theta}\right).\nabla C^k\right]-\nabla.\left(qC^k\right)-q_s^{\backslash}*C_s^k \quad [2]$$

where, $\boldsymbol{\rho_0}$: fluid density [ML^{-3}] at the reference concentration and temperature; $\boldsymbol{\mu}$: dynamic viscosity [$ML^{-1}\ T^{-1}$]; $\mathbf{K_0}$: hydraulic conductivity [LT^{-1}]; $\mathbf{h_0}$: hydraulic head [L], $\boldsymbol{\rho_b}$: bulk density [ML^{-3}], $\boldsymbol{\rho_s}$: density of the solid [ML^{-3}], $\mathbf{S_{s,\ 0}}$: specific storage [L^{-1}], $\mathbf{t}$: time [T]; $\boldsymbol{\theta}$: porosity [−]; $\mathbf{C}$: salt concentration [ML^{-3}], $\mathbf{q}$: specific discharge [LT^{-1}], $\mathbf{q_s^{\backslash}}$: a source or sink [$T^{-1}$], $\mathbf{D_m^k}$: is the molecular diffusion coefficient [L^2T^{-1}] for species k; $\boldsymbol{\alpha}$: is the dispersivity tensor [L]; $\mathbf{K_d^k}$: distribution coefficient of species k [$L^3\ M^{-1}$], $\mathbf{C^k}$: the concentration of species k [ML^{-3}], $\mathbf{C_s^k}$: the source or sink concentration [ML^{-3}], $\mathbf{C_{Psolid}}$: specific heat capacity of the solid [$L^2\ T^{-2}\ {}^{\circ}K^{-1}$].

2.2. Hypothetical model design

The SEAWAT model was first validated against the experimental results reported by Abdoulhalik and Ahmed (2017), who used a laboratory flow tank with a dimension of (x; y; z) 0.38 m × 0.15 m x 0.01 m (Fig. 1a). The tank was subdivided into three distinct compartments: a central chamber and two reservoirs on either side. The central chamber was used to simulate the cross-section of an unconfined coastal aquifer. Clear glass beads were used to simulate the porous medium. The central chamber was isolated from the two side reservoirs by two fine mesh acrylic screens with an aperture diameter of 0.5 mm located at each side (Abdoulhalik and Ahmed 2017; Abdoulhalik et al., 2024). The aperture of these meshes was small enough to contain the glass beads and sufficiently large to allow the circulation of water flowing from the side reservoirs.

For each study, the dimensions of the two-dimensional vertical simulation area corresponded to the dimensions of the porous media chamber of the flow tank. The model domain was evenly discretized with a grid size of 0.2 cm. A no-flow boundary condition was set at the top and bottom of the model domain. The longitudinal dispersivity was estimated after the trial-and-error process. It was eventually estimated at 0.1 cm, and the transverse dispersivity was 0.05 cm, which is within the range of dispersivity values reported by Abarca and Clement (2009). All the numerical simulations neglected molecular diffusion (Riva et al., 2015). The specific storage was set at 10^{-6} cm^{-1}. The freshwater density was 1000 g/L, and the saltwater density was 1025 g/L. Considering the standard density-concentration slope factor of 0.7, a concentration of 36.16 g/L was used for the seawater boundary (Table 1).

The model simulated the subsurface dam and the cut-off wall by changing the hydraulic conductivity in the cells of interest to 10 cm/min for a permeable barrier. In contrast, the hydraulic conductivity of 1×10^{-5} cm min^{-1} was assigned for impermeable barriers. The cut-off wall depth and width are 134 mm and 20 mm, respectively, with 66 mm from the seaside, while the cut-off wall height is 70 mm and 24 mm in width and 20 mm from the seaside.

At the start of the simulation, the model domain corresponded to an entirely fresh aquifer. Freshwater and saltwater boundaries were initially set to 13.57 cm and 12.97 cm, respectively, allowing saline water to penetrate the model domain until it reached a steady state (Table 1).

On the other hand, there are 12 cases of mixed physical subsurface barriers (MPB) configurations applied using impermeable ($k = 1 \times 10^{-5}$ cm/min) and permeable hydraulic conductivity (k = 10 cm/min). All MPB configurations were tested for homogeneous aquifer (k = 85 cm/min) and layered heterogeneous aquifer composed of three layers with hydraulic conductivity of 85 cm/min, 17 cm/min, and 85 cm/min from top to bottom, respectively. The variables used are presented in Table 2.

On top of the base case that has no barrier, we considered the following three cases.

I. The first (case I) is a cut-off wall located at the land side and the subsurface dam at the seaside (Fig. 1b) and
II. The second (case II) is the subsurface dam located at the land side and the cut-off wall located at the seaside (Fig. 1c) and
III. III. The third (case III) is the two walls were located on top of each other (Fig. 1d).

3. Results

3.1. Simulation of the base case

Fig. 2 presents the results of the current model using SEAWAT code for the base case at homogenous (Fig. 2a) and heterogeneous cases (Fig. 2b). The freshwater head was decreased to impose a head

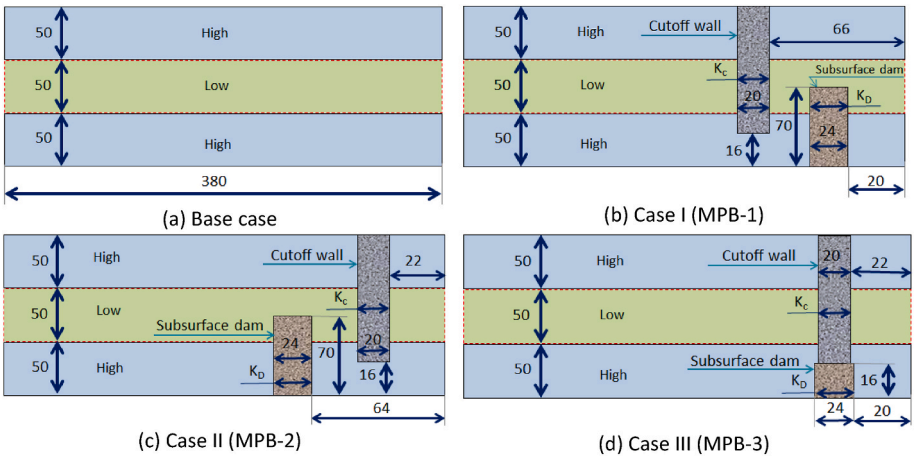

Fig. 1. The schematic design of the MPB configuration has dimensions in mm.

Table 1
Boundary conditions and hydraulic parameters of study cases.

Parameters	Value	Unit
Boundary conditions		
Inland freshwater (h_f)	13.57	cm
Saltwater head (h_s)	12.97	cm
Landside freshwater concentration (C_f)	0	gm L^{-1}
Seaside saltwater concentration (C_s)	36.60	gm L^{-1}
Initial concentration (C_0)	1	gm L^{-1}
Hydraulic parameters		
Hydraulic conductivity (k) (Isotropic) for top and bottom layers	85	cm min^{-1}
Hydraulic conductivity (k) (Isotropic) for middle layer	17	cm min^{-1}
Porosity (n)	0.30	–
Freshwater density (ρ_f)	1000	gm L^{-1}
Saltwater density (ρ_s)	1025	gm L^{-1}
Specific Storage	10^{-6}	cm^{-1}
Longitudinal dispersivity (α_L)	0.10	cm
Transverse dispersivity (α_T)	0.05	cm
Molecular diffusion coefficient(D*)	0	m^2 day^{-1}
Recharge	0	mm $year^{-1}$

Table 2
Different MPB configurations for homogenous and heterogeneous aquifers.

Barrier Configuration	Case	Cut-off Wall		Subsurface Dam	
		Location	Hydraulic Conductivity (K_W) (cm/min)	Location	Hydraulic Conductivity (K_D) (cm/min)
MPB-1	**1**	Landside	1×10^{-5}	Seaside	10
	2		10		$1*10^{-5}$
MPB-2	**3**	Seaside	1×10^{-5}	Landside	10
	4		10		$1*10^{-5}$
MPB-3	**5**	Seaside	1×10^{-5}	Seaside	10
	6		10		$1*10^{-5}$

difference dh = 4 mm, corresponding to a hydraulic gradient of 0.0105. The intrusion of the 0.5 isochlor reached 24.10 cm and 23 cm from the seaside for the homogenous and heterogeneous, respectively. The SEAWAT results were compared with the experimental results, as presented in Fig. 2c for the homogenous case and Fig. 2d for the heterogeneous case. The comparison shows a good agreement between the SEAWAT model results and the experimental results of Abdoulhalik and Ahmed (2017a).

Also, the results of groundwater heads and velocities distribution are shown in the Appendix for Figure A1a (homogenous case) and Figure A1b (heterogeneous). The groundwater heads ranged from 12.95 cm at the landside to 13.35 cm at the sea. The seawater wedge was smoothly curved in the homogeneous case while it was refracted at the layers interface for the layered heterogeneous aquifer.

3.1.1. Case MPB-1: cut-off wall located at the land side and subsurface dam at the seaside

Two different configurations were applied for this case: MPB-1, where the cut-off wall is on the land side, and the subsurface dam is on the seaside. The two configurations are (1) the cut-off wall was impermeable while the dam was permeable, and (2) the cut-off wall is permeable while the dam is impermeable. In these two configurations, a permeable barrier (wall or dam) has a permeability of 10 cm/min, while an impermeable barrier has a permeability of 1×10^{-5} cm/min. Both configurations were examined for homogenous (Fig. 3a and b) and heterogeneous (Fig. 3c and d) aquifers, respectively.

The MPB-1 results showed that the intrusion length reached 7.20 cm (Figs. 3a) and 4.20 cm (Fig. 3b), compared with 24.10 cm for the homogenous case when there was no physical barrier. The Results indicated that the most effective position of MPB-1 occurred when the dam was impermeable while the cut-off wall was permeable (Fig. 3b). This case has the best reduction in the SWI wedge. The groundwater heads and velocity distribution for these two cases are presented in the Appendix (Figures A2a and A2b) for homogenous cases. Indeed, the impermeable dam case had repulsed the seawater wedge back where the freshwater flow, especially between the wall and the wedge, was high enough to push the seawater back toward the seaside and hence produced better seawater wedge reduction than the other case when the dam was permeable, and the wall was impermeable.

Fig. 3c and d shows the impact of the MPB-1 barrier configurations on the SWI wedge for the layered heterogeneous aquifer. The case of the impermeable dam and permeable cut-off proves again to be effective in mitigating SWI and pushing the seawater wedge back into the seaside of the wall. Like the homogeneous aquifer, the seawater wedge stayed at the seaside and did not spill over the dam to the other side. The freshwater flow for this configuration was high enough to stop the wedge short and prevent it from progressing into the landside of the barrier. It can be noted that the seawater wedge was shorter for this layered aquifer than the homogenous aquifer for the same barrier configuration. The intrusion length reached 7 cm for the impermeable cut-off wall and permeable dam configuration and 3.60 cm for the permeable cut-off wall and impermeable dam configuration, compared with 23 cm in the base case without any barrier installed.

Moreover, Figures A2c and A2d in the Appendix present the distribution of groundwater heads and velocity at heterogeneous aquifers.

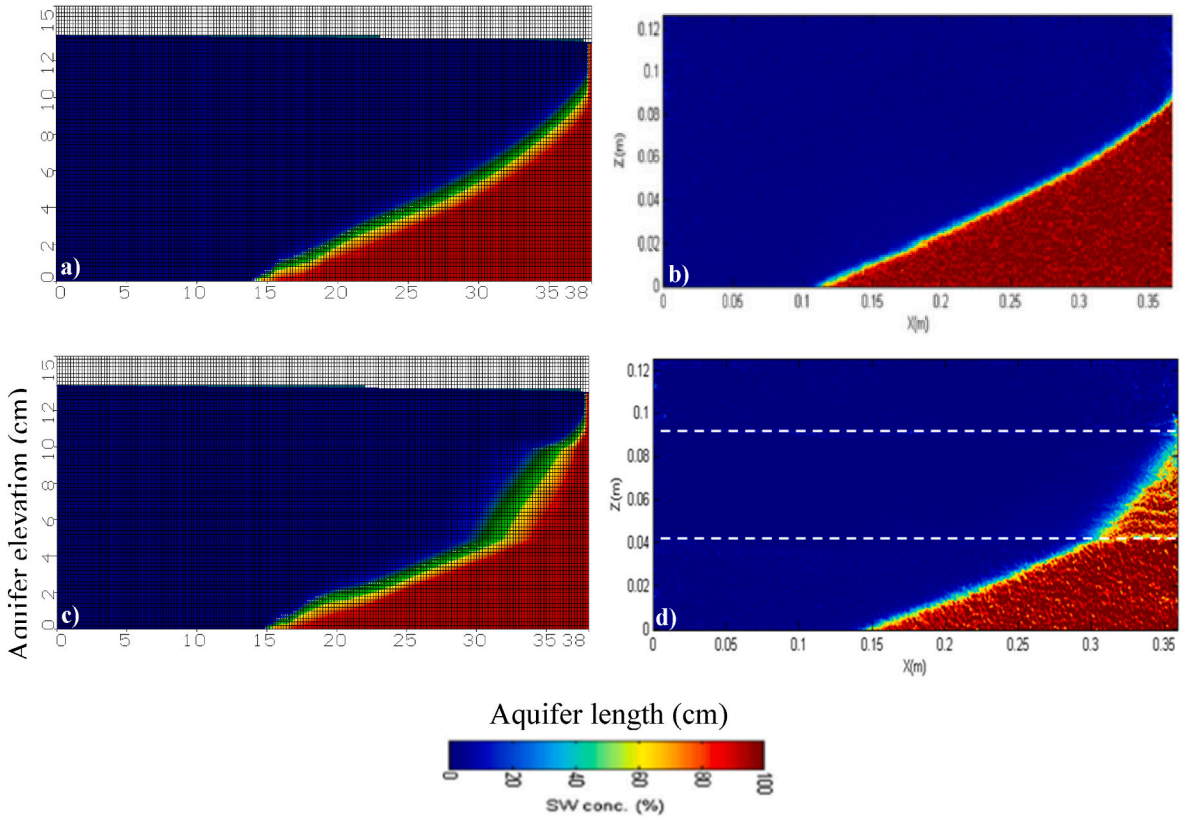

Fig. 2. Salinity results obtained by SEAWAT for a) homogenous cases, (b) experimental for homogenous cases (Abdoulhalik and Ahmed, 2017a), c) heterogeneous case, and d) Experimental for the heterogeneous case (Abdoulhalik and Ahmed, 2017a),.

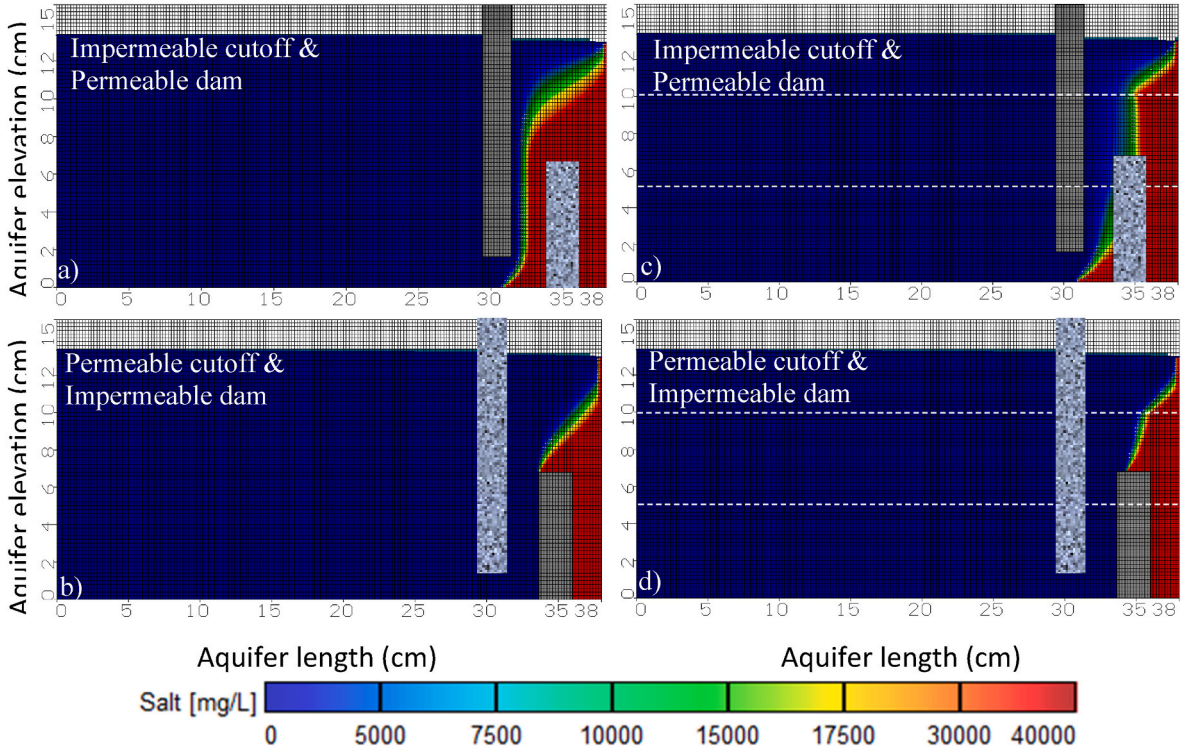

Fig. 3. SWI distribution for a cut-off wall at the land side and the subsurface dam at the seaside (MPB-1), the homogenous case (left), and the heterogeneous case (right).

The minimum SWI occurred using MPB-1 with a permeable cut-off wall and impermeable dam, which is also the best position for MPB in Figure A2d due to the reduction of wall length. Also, the results showed that using a permeable cut-off wall at the land side and an impermeable subsurface dam at the seaside in heterogeneous aquifers is effective for mitigating the SWI in coastal aquifers compared with other cases.

3.1.2. *Case MPB-2: cut-off wall located at the seaside and subsurface dam at the landside*

Like the previous case, two configurations were considered for MPB-2; these are (1) the cut-off wall was impermeable while the dam was permeable, and (2) the cut-off wall is permeable while the dam is impermeable. Again, in these two configurations, a permeable barrier has a 10 cm/min permeability, while an impermeable barrier has a 1×10^{-5} cm/min permeability. Both configurations were examined for homogenous (Fig. 4a and b) and heterogeneous aquifers (Fig. 4c and d), as in the above case of MPB-1.

For the homogeneous aquifer, Fig. 4a and b shows that the MPB-2 reduced the intrusion length such that the seawater wedge reached 4.2 cm and 6.5 cm, respectively, compared with 24.1 cm in the base case. Thus, for the MPB-2 case, the scenario of an impermeable cut-off wall and permeable dam reduced the saltwater wedge to 4.2 cm compared with 7.2 cm in the case of MPB-1 for the same scenario. This means the MPB-2 configuration produced a greater reduction in the seawater wedge when the dam was permeable and the cut-off wall was impermeable. On the other side, an impermeable dam and permeable cut-off wall scenario was not as effective in the MPB-2 configuration as it was in the MPB-1 configuration. This impermeable dam and permeable cut-off wall increased the wedge to 6.5 cm in the MPB-2 configuration compared with 4.20 cm in the MPB-1 configuration.

A similar MPB-2 effect was observed for the heterogeneous aquifer (see Fig. 4c and d). For the impermeable cut-off wall and permeable dam (Fig. 4c), the wedge length was 5.8 cm, which is as good as the case MPB-1, where the wedge length was 7 cm in the same MPB-1 configuration. However, for the other scenario (Fig. 4d), the permeable cut-off wall and impermeable subsurface dam configuration, the seawater wedge was reduced to 6.5 cm compared with 3.6 cm in the case of MPB-1 for the same scenario, which is the same reduction produced in the homogeneous aquifer (6.5 cm) of It should be noted here that all these reduction values in the seawater wedge are still significant compared with the wedge length of 24.1 cm, and 23 cm in the base case scenario for the homogenous and layered aquifers, respectively.

Figures A3a to A3d in the Appendix show the distribution of groundwater heads and velocity; the figures show a decrease in the freshwater flux. Figures A3a and A3c show that the permeability of the dam was not small enough to prevent the freshwater from traveling through it completely. However, it helped partially to refract the freshwater flow. It forced it to flow into the opening between the dam and the wall, which significantly reduced the saltwater wedge and forced it back toward the seaside.

3.1.3. *Case MPB-3: cut-off wall placed above the dam*

In this case, MPB-3, both the cut-off wall and the dam are installed above each other. Similar to the previous two cases, MPB-1 and MPB-2, we studied here the scenario when the wall was impermeable ($k = 1 \times 10^{-5}$ cm/min) while the dam permeable ($k = 10$ cm/min), and also the opposite scenario where the wall was permeable while the dam was impermeable. Again, the modeling covered both homogeneous and layered aquifers (Fig. 5).

Fig. 5a and b shows the MPB-3 results for the homogeneous aquifer. They indicate a decrease in the intrusion wedge length from the shoreline, reaching 2.60 cm in Fig. 5a for the impermeable cut-off wall and permeable dam configuration. In comparison, it reached 2.10 cm for the permeable cut-off wall and impermeable dam configuration in Fig. 5b. These values are compared with a wedge length of 24.10 cm in the base case when no barrier was installed. Apparently, this configuration produced the most reduction in the seawater wedge, reaching 89% and 91% for the two cases, respectively. It confirms that when the impermeable cut-off wall is placed on top of the permeable dam configuration, the seawater wedge produces the most significant reduction.

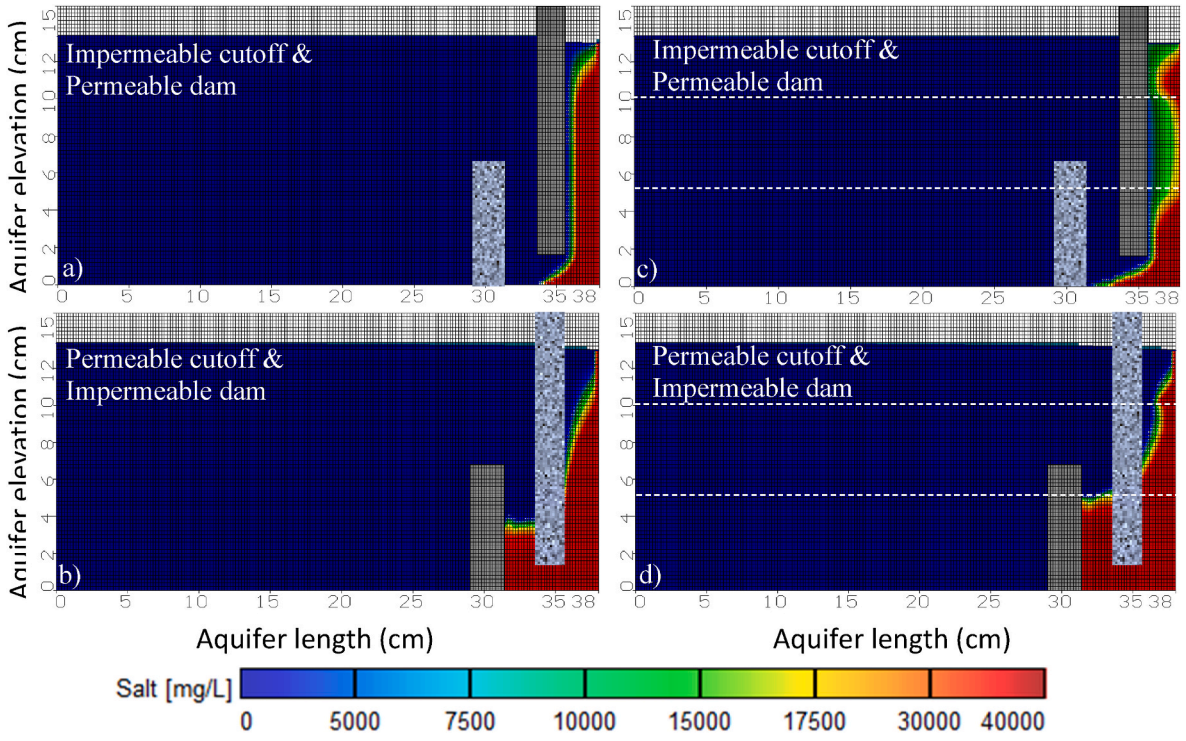

Fig. 4. SWI distribution for a cut-off wall at the land side and the subsurface dam at the seaside (MPB-1), the homogenous case (left), and the heterogeneous case (right).

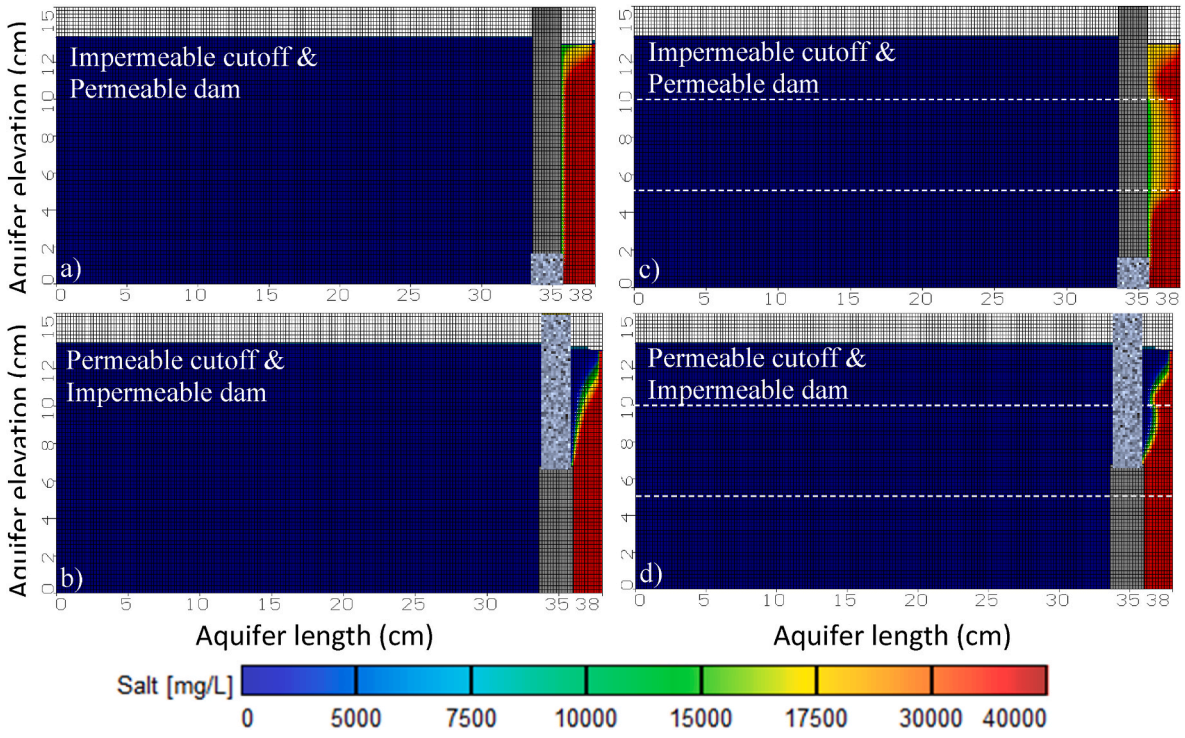

Fig. 5. SWI distribution for the cut-off wall and the subsurface dam at the seaside (MPB-3), the homogenous case (left), and the heterogeneous case (right).

Fig. 5c and d presents the results of MPB-3 for the layered aquifer setting of barrier configuration. The results showed that the intrusion length reached 2.60 cm (Fig. 5c) for the case when the impermeable cut-off wall was placed on top of the permeable dam and 1.85 cm (Fig. 5d) for the scenario when the permeable cut-off wall was placed on top of the impermeable dam. These wedge lengths are compared with a wedge of 23 cm in the base case when no barrier existed. These results suggest a wedge reduction of 89% when an impermeable cut-off wall was placed on top of the permeable dam and 92% when the permeable cut-off wall was placed on top of the impermeable dam. These are great reductions in the seawater wedge and show this MPB-3 configuration is the most effective in reducing the seawater wedge.

The distribution of groundwater heads and velocity are presented in Figures A4c to A4d in the Appendix. The low cost of the wall construction using MPB-3 at the permeable cut-off wall and impermeable subsurface dam at the seaside (Figure A4d) due to the minimum length. Moreover, Figure A4d presents the best position for MPB for the two walls at the seaside in the heterogeneous case due to the reduction of wall height and construction cost.

3.2. *Application to field study for Biscayne Aquifer, Florida state, USA*

The results for the hypothetical case study were validated using Biscayne in the Broward County Estate in southeast Florida, USA. The Biscayne aquifer is located between 25° 36″ and 25° 38″ North, 80° 17″ and 80° 20″ West (see Fig. 6); it is the main source of drinking water and the primary source of irrigation water for agriculture in Miami-Dade County (Langevin et al., 2020; Tully et al., 2019). Global climate change is likely to alter many environmental conditions in Florida, and the resulting changes may affect the natural characteristics of the state's fresh and coastal waters (Haque, 2023).

The field case study is the Biscayne aquifer in the Broward County Estate of Southeastern Florida, USA. The model domain was set up using a length of 22800 m, a depth of 105 m, and a width of 15 m. Fig. 7a

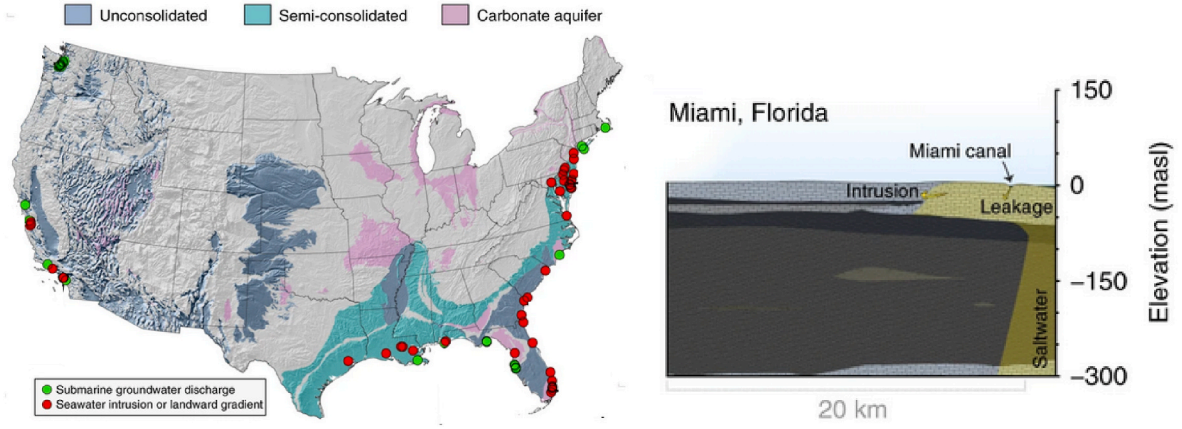

Fig. 6. Biscayne Aquifer, Florida, USA (left) near Miami (Renken et al., 2005; Prinos et al., 2014), a shallow carbonate aquifer (Biscayne) has experienced seawater intrusion, likely exacerbated by the construction of leaky canals (right) after (Jasechko et al., 2020).

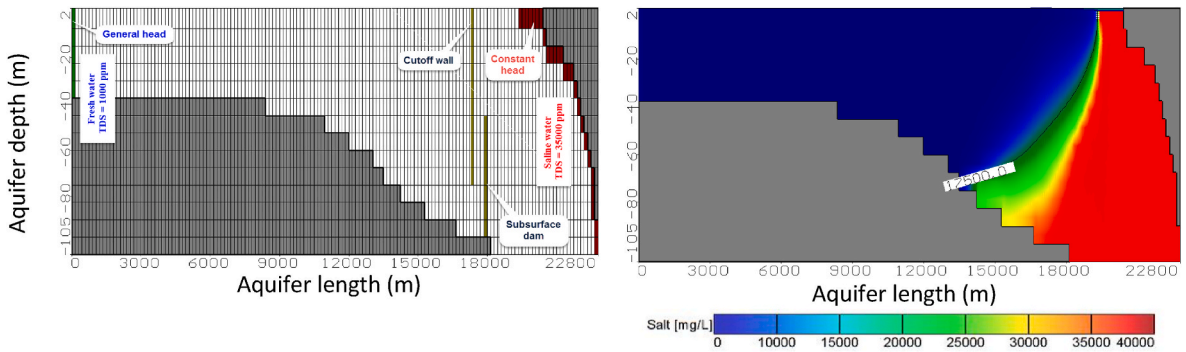

Fig. 7. Biscayne aquifer for a) boundary conditions and b) salinity results by SEAWAT for distribution of 0.5 isochlor (17500 ppm) at the baseline case (without management).

shows the domain, including 152 columns and 14 layers, with cell dimensions of 150 m × 150 m x 7.50 m (Δx*Δz*Δy), respectively. The main hydraulic parameters of the Biscayne aquifer were taken from Dausman and Langevin (2002), and the recharge of the aquifer was 254 mm year^{-1}. The freshwater density (ρ_f) is 1000 kg/m^3, saltwater density (ρ_s) is 1025 kg/m^3, horizontal hydraulic conductivity (K_h) is 1150 m/day, the vertical hydraulic conductivity (K_v) is 150 m/day. The aquifer porosity is 0.10; the storage is 1*10^{-5}; the Longitudinal dispersivity (α_L) is 3 m; the Transverse dispersivity (α_T) is 0.30 m; the molecular diffusion coefficient (D*) is 0 m^2/day.

The boundary conditions at the seaside (left side) were assigned using a constant head of 0.308 m with a concentration by the total dissolved solids (TDS) of 35 kgm^{-3}, the aquifer side for the fresh groundwater (right side) was assigned using the inland flux by a general head of 2.12 m with a fresh groundwater concentration of 1000 kg/m^3.

Fig. 7b shows the simulation boundary conditions for the study area using SEAWAT 4 under the steady state conditions for the Biscayne aquifer, where the intrusion reached 14 Km from the shoreline measured at the bottom of the aquifer.

The management scenarios were applied using a cutoff wall at 5400 m from the seaside and a depth of 77 m from the ground surface. The subsurface dam was installed at a distance of 4800 m from the sea side and a height of 52.50 m. The wall and dam hydraulic conductivity were variable based on the study scenario where the low or (impermeable)

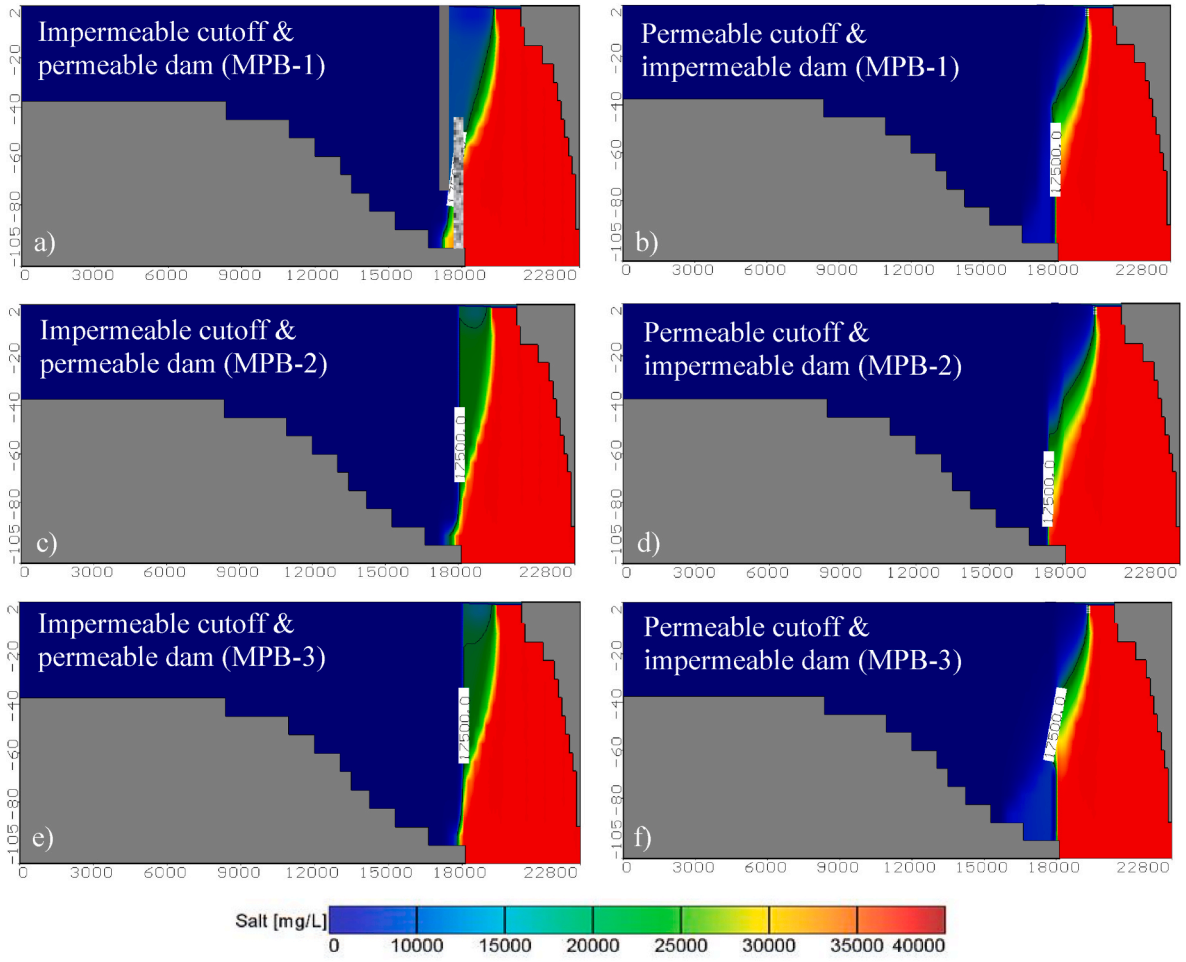

Fig. 8. SWI distribution for using the cut-off wall and the subsurface dam for the Biscayne aquifer for different configurations.

hydraulic conductivity is 144 m/day while the high (permeable) hydraulic conductivity is 1×10^{-5} m/day.

The results showed that for MPB-1 using an impermeable cutoff wall located at the land side and a permeable subsurface dam at the seaside, the SWI reached 5.57 km from the seaside (Fig. 8a). In comparison, the aquifer intrusion reached 4.89 km by applying a permeable wall and impermeable dam (Fig. 8b). For the configuration MPB-2, the SWI reached 5.14 km for using the impermeable wall located at the seaside and the permeable dam at the land side (Fig. 8c). Also, the SWI reached 5.4 km using the permeable wall and impermeable dam (Fig. 8d). Moreover, with the use of MPB-3 configuration, the two walls and dam were located at the seaside, and the intrusion reached 4.90 km using the impermeable wall and the permeable dam (Fig. 8e). In contrast, the intrusion reached 4.73 km for the application of the permeable wall and the impermeable dam (Fig. 8f).

4. Discussion

The results of this study provide important insights into the effectiveness of different mixed physical barriers (MPBs) in controlling seawater intrusion (SWI) in both homogeneous and heterogeneous aquifers.

The baseline scenario without physical barriers showed that the SWI in a homogeneous aquifer extends further inland (24.10 cm) than in a heterogeneous aquifer (23 cm). This small difference underlines the influence of aquifer heterogeneity on SWI dynamics. The curvature of the seawater wedge in the homogeneous aquifer and its refraction at the layer boundaries in the heterogeneous aquifer illustrate the complexity caused by the geological heterogeneity.

Three different configuration cases for MPB included: (1) the cut-off wall at the land side and the subsurface dam at the seaside (MPB-1), (2) the subsurface dam at the land side and the cut-off wall at the seaside (MPB-2), and (3) the cut-off wall is placed above the dam such that they were vertically above each other (MPB-3). Also, the study examined alternating cases of the permeable cut-off wall with the permeable dam scenario and then an impermeable cut-off wall with a permeable dam scenario. This has produced together 12 different configurations of mixed physical barriers that we investigated in this study in addition to the base case as in Table 2.

In the MPB-1 configuration, the placement of an impermeable dam at the seaside and a permeable cut-off wall at the landside proved to be the most effective arrangement for both homogenous and heterogeneous aquifers. Namely, in the first for MPB-1, the use of an impermeable cut-off wall and permeable dam helped reduce the SWI wedge by 70% and 71% for the homogenous and heterogeneous cases, respectively (Table 3 and Fig. 9a). Table 3 presents the reduction in the seawater wedge for all the different barrier configurations and its percentage compared with the base case.

For the same homogenous case, the field case study of the Biscayne aquifer in the Broward County Estate of Southeastern Florida, USA, was applied to investigate the intrusion under different wall configurations. The intrusion reduced the seawater wedge by 36% and 44%, as presented in Fig. 9b. Both the hypothetical case and real case study showed the same trend for increasing the % of salinity removed from the groundwater aquifers.

The use of a permeable cut-off wall and impermeable subsurface dam reduced the SWI by 83% and 85% for the homogenous and heterogeneous cases, respectively (Table 3 and Fig. 9a). Thus, the MPB-1 configuration of a permeable cut-off wall and impermeable subsurface dam provided better control of the saline wedge for both homogenous and layered aquifers. The significant decrease in SWI intrusion length demonstrates the efficacy of this barrier setup in promoting freshwater flow and repelling seawater.

The MPB-2 configuration, with the cut-off wall at the seaside and the subsurface dam at the landside, also showed effectiveness in mitigating SWI. However, its performance varied compared to MPB-1. Namely, for MPB-2, the use of an impermeable cut-off wall and permeable subsurface dam reduced the seawater wedge by 83% and 76% for homogenous and layered aquifers, respectively, and 73% for permeable cut-off wall with an impermeable subsurface dam for both aquifer types respectively, compared with the base case without using mix physical barriers, as shown in Table 3 and Fig. 9a. This indicates that placing impermeable barriers closer to the seaside is generally more effective. In the heterogeneous aquifer, similar trends were observed, but the effectiveness was slightly reduced compared to the homogeneous case, suggesting that aquifer heterogeneity impacts the optimal MPB placement.

Table 3
Results of using Mixed physical barriers for SWI length and repulsion percentage.

Physical Barriers	Case	Homogeneous		Heterogeneous	
	Barrier Configuration	SWI Length (cm)	SWI Repulsion (%)	SWI Length (cm)	SWI Repulsion (%)
Baseline		24.1	–	23	5
Cut-off wall located at the land side and subsurface dam at the seaside **(MPB-1)**	Impermeable wall & permeable dam	7.2	70	7	71
	Permeable wall & impermeable dam	4.2	83	3.6	85
Cut-off wall located at the seaside and subsurface dam at the landside **(MPB-2)**	Impermeable wall & permeable dam	4.2	83	5.8	76
	Permeable wall & impermeable dam	6.5	73	6.5	73
Cut-off wall placed above the dam **(MPB-3)**	Impermeable wall & permeable dam	2.6	89	2.6	89
	Permeable wall & impermeable dam	2.1	91	1.85	92

For the Biscayne aquifer, the installation of MPB-2 reduced the seawater wedge by 41% and 38%, as presented in Fig. 9b. The results showed agreement between the hypothetical case and the real case for the optimal MPB configuration.

Finally, the MPB-3 configuration, where the cut-off wall and subsurface dam are stacked, showed the highest reduction in SWI wedge length. Regarding the MPB-3, the results in Table 3 and Fig. 9a show the configuration of an Impermeable cut-off wall and permeable subsurface dam decreased the SWI by 89% for both aquifer types. For the other configuration of permeable cut-off wall and impermeable dam, the reduction in the seawater wedge reached 91% and 92% for homogeneous and heterogeneous layered aquifers, respectively, highlighting its potential as the most effective strategy for managing SWI in diverse aquifer conditions. The groundwater head and velocity distributions provided additional insights into the dynamics of SWI under different barrier configurations. The higher freshwater flow rates in the scenarios with impermeable dams and permeable walls facilitated the repulsion of the seawater wedge. This is particularly evident in the MPB-1 and MPB-3 configurations, where the permeability contrast between the barriers optimized the flow patterns to manage SWI effectively.

For the case of using MPB-3 in the real case of the Biscayne aquifer, the seawater wedge was reduced by 43% and 46%, as presented in Fig. 9b. A good agreement results and trends between the hypothetical case and real case for removing SWI in coastal aquifers.

These results agree with Abdoulhalik et al. (2017, 2024), who investigated MPB for homogeneous and layered heterogeneous aquifers.

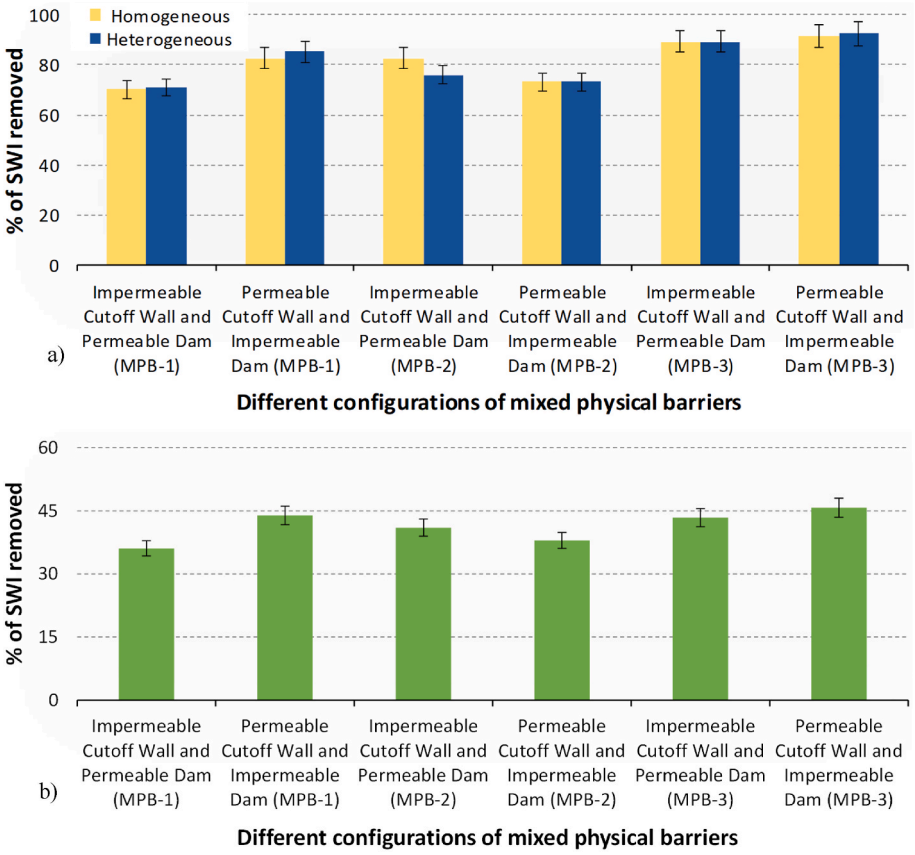

Fig. 9. The % of salt removed in the homogenous and heterogeneous cases for three MPB cases for a) hypothetical case and (b) Biscayne aquifer.

They used a mixed physical barrier composed of an impermeable cut-off wall and a semi-permeable subsurface dam. Chang et al. (2019)indicated that the subsurface dam blocks groundwater movement toward the sea. This blockage often accumulates pollutants and salts around the dam, which is intended for SWI at the seaside. However, it is not desired on the land side as it poses a serious problem in groundwater management. In our study, the existence of a permeable cut-off wall or dam in the configurated investigated here allowed the groundwater to pass through the permeable barrier, which acts like a connection between the aquifer and the sea with groundwater flow and improves the ecological environment in coastal areas.

Furthermore, Chang et al. (2019) explained that the single cut-off walls are unsuitable for coastal aquifers with low hydraulic gradients due to a decrease in the fresh groundwater heads. However, this new method of MPB configuration is good for increasing the fresh groundwater heads. The construction cost of this method is lower than barriers that have a single cut-off or dam, as demonstrated by Abdoulhalik et al. (2017). The reasoning provided by their study was that an MPB barrier with 40% wall depth produced 13% greater seawater reduction than a single cut-off wall that has a depth of 90% of the aquifer thickness. The single PSBs need 90% of the aquifer depth. Likewise, the permeable part could reduce the cost of this method in coastal aquifers. The semi-permeable dam could be effective in deep aquifers due to the construction of the lower parts of the aquifer (Abd-Elaty and Zelenakova (2022). Our findings also agree with Wang et al. (2023), who studied the impact of using mixed barriers on SWI and nitrate accumulation in coastal unconfined aquifers. The results showed that the degree of nitrate accumulation increased linearly with the cut-off wall's height. Under certain conditions, MPB was 46–53% and 16–57% more efficient in preventing and controlling SWI than conventional subsurface dams and cut-off walls. However, MPB caused 14–27% and 2–12% more nitrate accumulation than the subsurface dam and cut-off wall. The results of this study have practical implications for the design and implementation of SWI mitigation strategies. The effectiveness of MPB configurations in both homogeneous and heterogeneous aquifers suggests that customized barrier configurations can be developed to address specific geologic and hydrologic conditions. In particular, the MPB-3 configuration offers a promising solution due to its superior performance in reducing SWI. Further research is needed to investigate the long-term sustainability and economic feasibility of these barrier configurations under different climate conditions and sea level rise scenarios. In addition, real-world case studies and field applications would provide valuable data to validate the model results and refine the guidelines for barrier design. Comparative studies with different SWI mitigation methods could also help to identify the most cost-effective and environmentally sustainable solutions for coastal aquifer management.

The settings of the numerical model limit the results and conclusions of this study. For example, if the boundary conditions for the inland are dynamic, the results may vary (Wu and Lu, 2023). Other studies have emphasized that the dimensions (2D or 3D) of the model can also significantly influence the effectiveness of the barrier (Kaleris and Ziogas, 2013; Wu et al., 2020). Moreover, the limitations of the present study of using the MPB to control seawater intrusion include the financial implications of construction, such as subsurface barriers under the ground, which pose a real challenge, particularly when the aquifers are deep. Also, the application of this method for using different configurations of mixed physical barriers on a heterogeneous field scale is required to confirm the current numerical modeling results; it will yield more implications from a realistic perspective.

5. Conclusions

This study investigated the different configurations of mixed

subsurface physical barriers used to control seawater intrusion in coastal aquifers, covering homogeneous and layered heterogeneous aquifers. The MODFLOW family code SEAWAT was used for the simulations. The following conclusions may be drawn from this study.

1. When the cut-off wall was located directly above the subsurface dam, this produced the most effective configuration for controlling seawater intrusion (case MPB-3). The saltwater wedge reduction reached 91% and 92% for the homogeneous and layered heterogeneous aquifers, respectively. And it happened when the subsurface dam was impermeable while the cut-off wall directly above it was porous. The other alternating configuration, i.e., when the cut-off wall was impermeable and the dam was permeable, was also effective in this setting of mixed barrier in which the saltwater wedge reduction reached 89% for both aquifers.
2. When the cut-off wall was located at the landside while the dam was at the seaside, this configuration was also effective and produced great wedge reduction (case MPB-1). The best scenario for this mixed barrier configuration was when the dam was impermeable while the cut-off wall was permeable. For this scenario, the seawater wedge reduction reached 83% and 85% for the homogeneous and layered heterogeneous aquifers, respectively.
3. Placing the cut-off wall at the seaside while the dam was at the landside produced the least effective configuration in reducing seawater intrusion compared to the above two configurations (case MPB-2). However, the overall seawater wedge reduction of this configuration is still significant. The wedge reduction reached 83% and 76% for the homogeneous and layered heterogeneous aquifers, respectively, and it happened when the cut-off wall was impermeable while the dam was permeable.
4. The homogenous field case study of the Biscayne aquifer in the Broward County Estate of Southeastern Florida, USA, was applied. The intrusion reduced the seawater wedge by 36% and 44% (case MPB-1), 41%, and 38% (case MPB-2), and 43% and 46% (case MPB-3).

This method effectively manages groundwater salinity, increases freshwater storage, and tackles groundwater pollutants with reactive filters. Compared to using the single PSBs method, it is particularly effective in areas with low groundwater heads caused by drought. Future research should consider, among others, the financial implications for the proposed configurations of mixed physical barriers to manage seawater intrusion. Moreover, the heterogeneous field scale application is required to confirm the current laboratory scale results.

Funding

This study did not receive any funding

Conflicts of interest/Competing interests

The authors declare no conflict of interest.

Availability of data and material

Upon request

Code availability

Upon request

Ethics approval

Not applicable

Consent to participate

Yes

Consent for publication

Yes

CRediT authorship contribution statement

Ismail Abd-Elaty: Writing – review & editing, Writing – original draft, Visualization, Validation, Supervision, Software, Resources, Project administration, Methodology, Investigation, Formal analysis, Data curation, Conceptualization. **Alban Kuriqi:** Writing – review & editing, Writing – original draft, Supervision. **Ashraf Ahmed:** Writing – review & editing, Writing – original draft, Funding acquisition.

Declaration of competing interest

The authors declare that they have no known competing financial interests or personal relationships that could have appeared to influence the work reported in this paper.

Data availability

No data was used for the research described in the article.

Acknowledgment

Ismail Abd-Elaty thanks the Department of Water and Water Structures Engineering, Faculty of Engineering, Zagazig University, Zagazig 44519, Egypt, for constant support during the study. Alban Kuriqi is grateful for the Foundation for Science and Technology's support through funding UIDB/04625/2020 from the research unit CERIS (https://doi.org/10.54499/UIDB/04625/2020).

Appendix

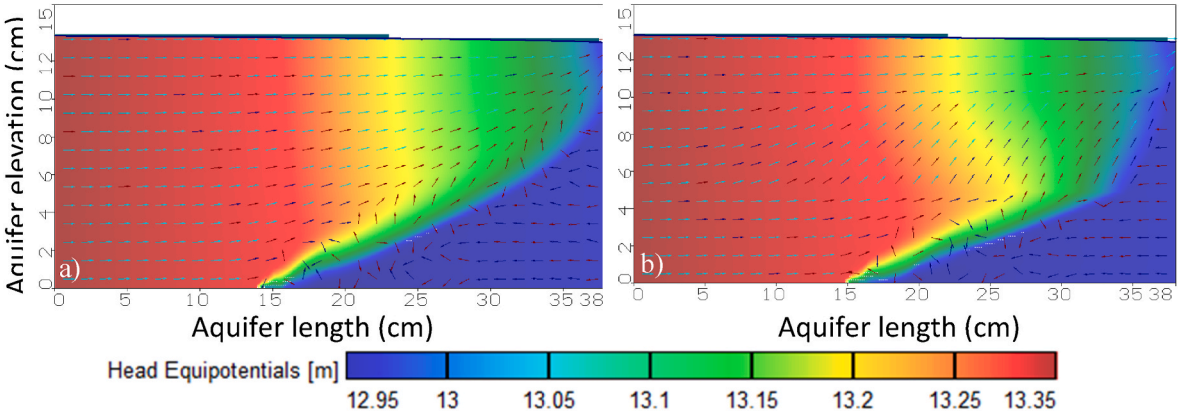

Fig. A1. Groundwater heads and velocity distribution results by SEAWAT at the base case for a) homogenous case and b) heterogeneous case.

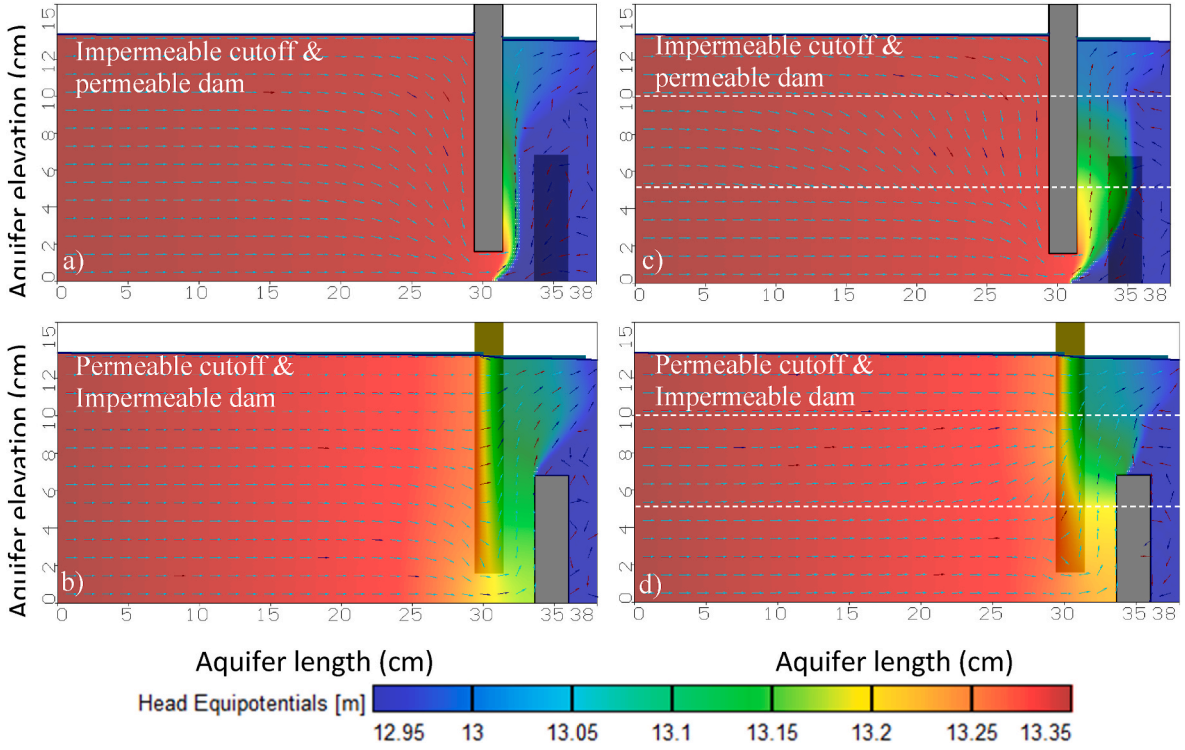

Fig. A2. Groundwater heads and velocity distribution for the cut-off wall at the land side and the subsurface dam at the seaside (MPB-1) cases, the homogenous case (left) and heterogeneous case (right).

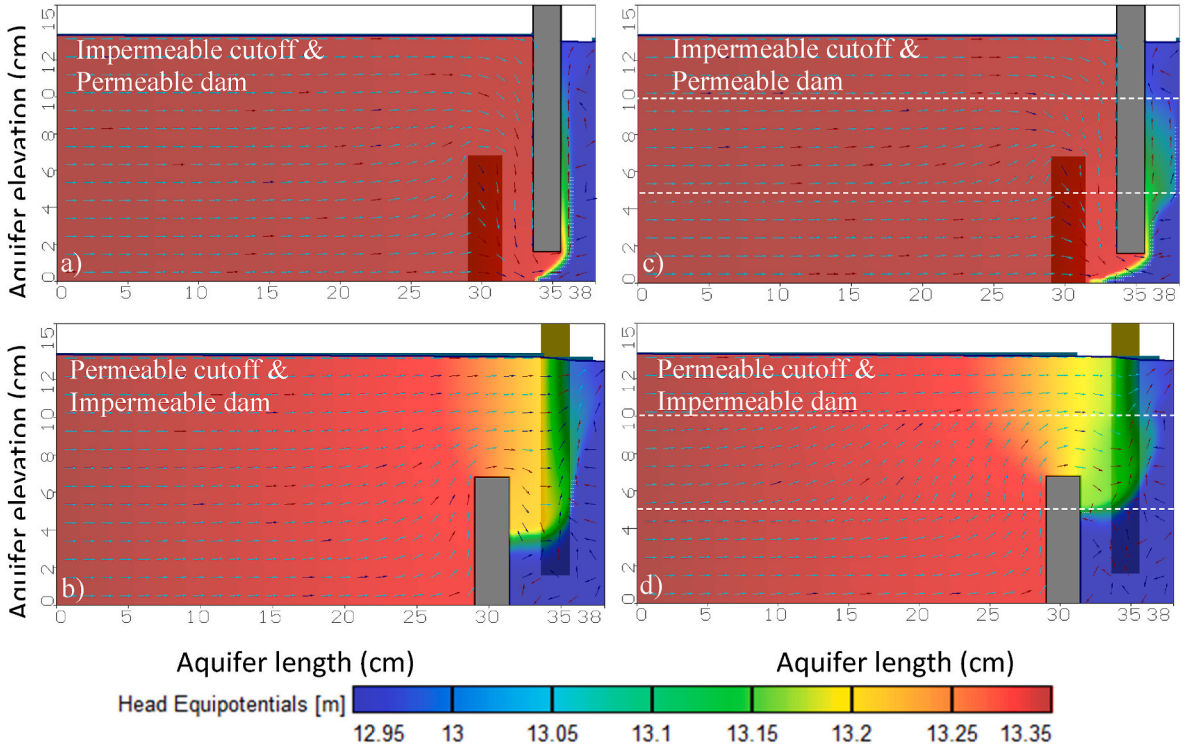

Fig. A3. Groundwater heads and velocity distribution for the cut-off wall at the land side and the subsurface dam at the seaside (MPB-1), the homogenous case (left), and the heterogeneous case (right).

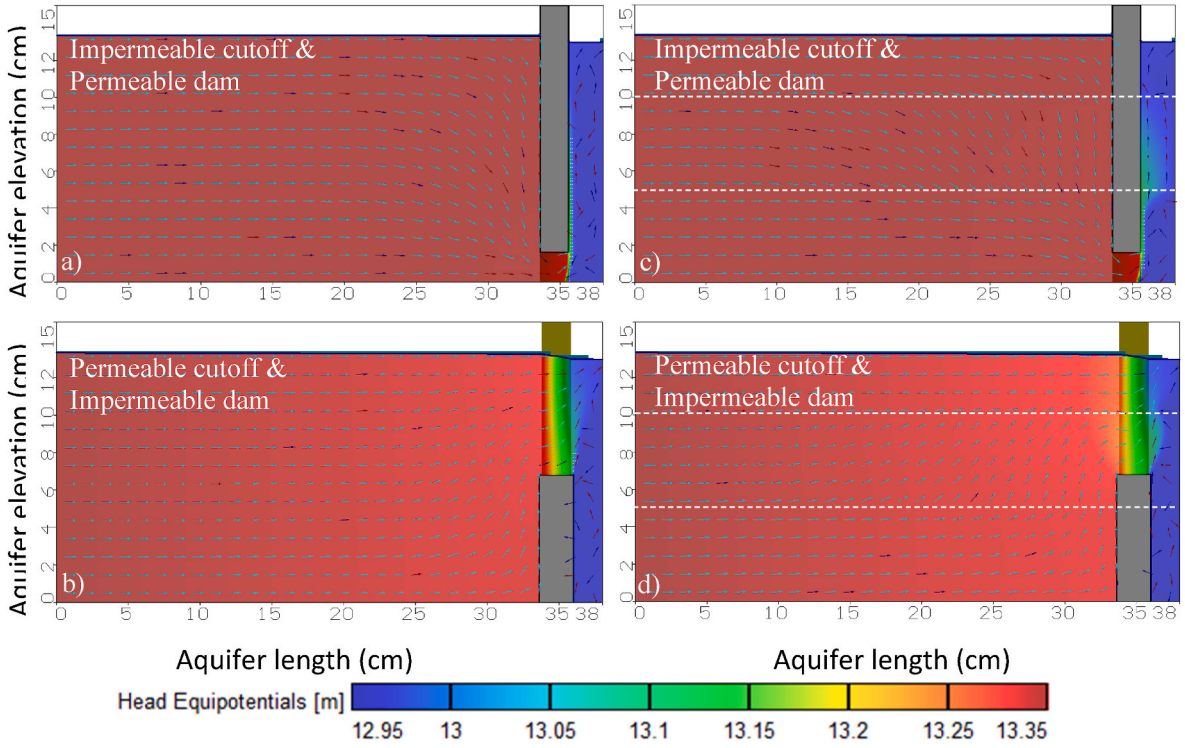

Fig. A4. Groundwater heads and velocity distribution for cut-off wall and the subsurface dam at the seaside (MPB-3), the homogenous case (left), and the heterogeneous case (right).

References

Abd-Elaty, I., Zelenakova, M., 2022. Saltwater intrusion management in shallow and deep coastal aquifers for high aridity regions. J. Hydrol.: Reg. Stud. 40, 101026.

Abd-Elaty, I., Kuriqi, A., Pugliese, L., et al., 2024. Shoreline subsurface dams to protect coastal aquifers from sea level rise and saltwater intrusion. Appl. Water Sci. 14, 49. https://doi.org/10.1007/s13201-023-02032-y.

Abdoulhalik, A., Ahmed, A.A., 2017a. The effectiveness of cutoff walls to control saltwater intrusion in multi-layered coastal aquifers: experimental and numerical

study. J. Environ. Manag. 199, 62–73. https://doi.org/10.1016/j.jenvman.2017.05.040.
Abdoulhalik, A., Ahmed, A.A., 2017b. How does layered heterogeneity affect the ability of subsurface dams to clean up coastal aquifers contaminated with seawater intrusion? J. Hydrol. 553, 708–721. https://doi.org/10.1016/j.jhydrol.2017.08.044.
Abdoulhalik, A., Ahmed, A., Hamill, G.A., 2017. A new physical barrier system for seawater intrusion control. J. Hydrol. 549, 416–427. https://doi.org/10.1016/j.jhydrol.2017.04.005.
Abdoulhalik, A., Ahmed, A.A., Abd Elaty, I., 2024. Effects of layered heterogeneity on mixed physical barrier performance to prevent seawater intrusion in coastal aquifers. J. Hydrol. https://doi.org/10.1016/j.jhydrol.2024.131343.
Allow, K.A., 2011. Seawater intrusion in Syrian coastal aquifers, past, present and future, case study. Arabian J. Geosci. 4, 645–653. https://doi.org/10.1007/s12517-010-0261-8.
Ashrafuzzaman, M., Santos, F.D., Dias, J.M., Cerdà, A., 2022. Dynamics and causes of sea level rise in the coastal region of southwest Bangladesh at global. Regional, and Local Levels 10, 779.
Chang, Q., Zheng, T., Zheng, X., Zhang, B., Sun, Q., Walther, M., 2019. Effect of subsurface dams on saltwater intrusion and fresh groundwater discharge. J. Hydrol. 576, 508–519. https://doi.org/10.1016/j.jhydrol.2019.06.060.
Dausman, A.M., Langevin, C.D., 2002. Representing hydrodynamic dispersion in saltwater intrusion models that differ in temporal resolution. American Water Resources Association, 2002 Spring Specialty Conference: Coastal Water Resources. New Orleans, Louisiana.
Haque, S.E., 2023. The effects of climate variability on Florida's major water resources. Sustainability 15 (14), 11364. https://doi.org/10.3390/su151411364.
Harne, S., Chaube, U.C., Sharma, S., Sharma, P., Parkhya, S., 2006. Mathematical modelling of salt water transport and its control in groundwater. Nat. Sci. 4, 32–39.
Jasechko, S., Perrone, D., Seybold, H., Fan, Y., Kirchner, J., 2020. Groundwater level observations in 250,000 coastal US wells reveal scope of potential seawater intrusion. Nat. Commun. 11, 3229. https://doi.org/10.1038/s41467-020-17038-2.
Kaleris, V.K., Ziogas, A.I., 2013. The effect of cutoff walls on saltwater intrusion and groundwater extraction in coastal aquifers. J. Hydrol. 476, 370–383. https://doi.org/10.1016/j.jhydrol.2012.11.007.
Langevin, C.D., 2001. Simulation of groundwater discharge to Biscayne Bay. southeastern Florida. USGS water-resources investigations report 00-4251, p. 137. https://fl.water.usgs.gov/PDF_files/wri00_4251_langevin.pdf.
Langevin, C.D., Panday, S., Provost, A.M., 2020. Hydraulic-head formulation for density-dependent flow and transport. Groundwater 58 (3), 349–362. https://doi.org/10.1111/gwat.12967.
Prinos, S.T., Wacker, M.A., Cunningham, K.J., Fitterman, D.V., 2014. Origins and Delineation of Saltwater Intrusion in the Biscayne Aquifer and Changes in the Distribution of Saltwater in Miami-Dade County. U.S. Geological, Florida, p. 116. Survey Report No. 2014-5025. https://pubs.er.usgs.gov/publication/sir20145025.
Renken, R.A., et al., 2005. Impact of Anthropogenic Development on Coastal Groundwater Hydrology in Southeastern Florida, 1900–2000, vol. 1275. U. S. Geol. Surv. Circular, p. 87. https://pubs.usgs.gov/circ/2005/circ1275/pdf/cir1275.pdf.
Rizzo, A., Vandelli, V., Gauci, C., Buhagiar, G., Micallef, A.S., Soldati, M., 2022. Potential Sea level rise inundation in the mediterranean: from susceptibility assessment to risk scenarios for policy action. Water 14, 416.
Tansel, B., Zhang, K., 2022. Effects of saltwater intrusion and sea level rise on aging and corrosion rates of iron pipes in water distribution and wastewater collection systems in coastal areas. J. Environ. Manag. 315, 115153 https://doi.org/10.1016/j.jenvman.2022.115153.
Tully, K., Gedan, K., Epanchin-Niell, R., Strong, A., Bernhardt, E.S., BenDor, T., Mitchell, M., Kominoski, J., Jordan, T.E., Neubauer, S.C., 2019. The invisible flood: the chemistry, ecology, and social implications of coastal saltwater intrusion. Bioscience 69, 368–378.
Wang, J., Kong, J., Gao, C., et al., 2023. Effect of mixed physical barrier on seawater intrusion and nitrate accumulation in coastal unconfined aquifers. Environ. Sci. Pollut. Res. 30, 105308–105328. https://doi.org/10.1007/s11356-023-29637-9.
Wu, H., Lu, C., 2023. Seasonal fluctuations in the groundwater level accelerate the removal of residual saltwater upstream of subsurface dams. J. Hydrol. 625, 130026 https://doi.org/10.1016/j.jhydrol.2023.130026.
Wu, H., Lu, C., Kong, J., Werner, A.D., 2020. Preventing seawater intrusion and enhancing safe extraction using finite-length, impermeable subsurface barriers: 3D analysis. Water Resour. Res. 56, e2020WR027792 https://doi.org/10.1029/2020WR027792.
Yu, Xuan, He, Lanxuan, Yao, Rongjiang, Tu, Tongbi, Zhang, Zebin, Zhao, Xinfeng, 2024. Effects of beach nourishment on seawater intrusion in layered heterogeneous aquifers. J. Hydrol. 633, 131018 https://doi.org/10.1016/j.jhydrol.2024.131018. ISSN 0022-1294.
Zheng, C., Wang, P.P., 1999a. MT3DMS: a Modular Three-Dimensional Multispecies Transport Model for Simulation of Advection, Dispersion, and Chemical Reactions of Contaminants in Groundwater Systems; Documentation and User's Guide.
Zheng, C., Wang, P.P., 1999b. MT3DMS: a Modular Three-Dimensional Multispecies Transport Model for Simulation of Advection, Dispersion, and Chemical Reactions of Contaminants in Groundwater Systems; Documentation and User's Guide.